THE JOURNAL OF BIOLOGICAL CHEMISTRY
Vol. 280, No. 28, Issue of July 15, pp. 26287–26294, 2005
Printed in U.S.A.

Ryanodine Receptors in Muscarinic Receptor-mediated Bronchoconstriction*

Received for publication, March 16, 2005, and in revised form, May 11, 2005
Published, JBC Papers in Press, May 13, 2005, DOI 10.1074/jbc.M502905200

Wanglei Du‡, Jonathan A. Stiber§, Paul B. Rosenberg§, Gerhard Meissner¶, and Jerry P. Eu‡‖

From the Divisions of ‡Pulmonary, Allergy and Critical Care Medicine and §Cardiology, Duke University, Medical Center, Durham, North Carolina, 27710 and ¶Department of Biochemistry and Biophysics, University of North Carolina, Chapel Hill, North Carolina 27599-7260

Ryanodine receptors (RyRs), intracellular calcium release channels essential for skeletal and cardiac muscle contraction, are also expressed in various types of smooth muscle cells. In particular, recent studies have suggested that in airway smooth muscle cells (ASMCs) provoked by spasmogens, stored calcium release by the cardiac isoform of RyR (RyR2) contributes to the calcium response that leads to airway constriction (bronchoconstriction). Here we report that mouse ASMCs also express the skeletal muscle and brain isoforms of RyRs (RyR1 and RyR3, respectively). In these cells, RyR1 is localized to the periphery near the cell membrane, whereas RyR3 is more centrally localized. Moreover, RyR1 and/or RyR3 in mouse airway smooth muscle also appear to mediate bronchoconstriction caused by the muscarinic receptor agonist carbachol. Inhibiting all RyR isoforms with ≥200 μM ryanodine attenuated the graded carbachol-induced contractile responses of mouse bronchial rings and calcium responses of ASMCs throughout the range of carbachol used (50 nM to ≥3 μM). In contrast, inhibiting only RyR1 and RyR3 with 25 μM dantrolene attenuated these responses caused by high (>500 nM) but not by low concentrations of carbachol. These data suggest that, as the stimulation of muscarinic receptor in the airway smooth muscle increases, RyR1 and/or RyR3 also mediate the calcium response and thus bronchoconstriction. Our findings provide new insights into the complex calcium signaling in ASMCs and suggest that RyRs are potential therapeutic targets in bronchospastic disorders such as asthma.

The three mammalian isoforms of ryanodine receptors (RyRs)[1] are large homotetrameric ion channels that constitute one of the two known families of intracellular Ca^{2+} release channels in eukaryotic cells (1, 2). These channels are so named because they bind specifically to the plant alkaloid ryanodine that was used to isolate them (3). RyRs and the other family of intracellular Ca^{2+} release channels, the inositol 1,4,5-trisphosphate receptors (IP_3Rs), may co-express in the same cell type (1, 4). These two families of ion channels mediate many cellular processes by releasing signaling messenger Ca^{2+} from intracellular stores into cytosolic compartments in response to extracellular stimuli (1).

The physiological roles and regulatory mechanisms of RyRs are best characterized in skeletal and cardiac muscles in which RyRs are essential for muscle contraction (4). RyR1 and RyR2 are the predominant RyR isoforms in skeletal and cardiac muscles, respectively. In these tissues, RyRs are localized to specialized regions of sarcoplasmic reticulum (SR) juxtaposing tubular invaginations of cell membrane known as t-tubules. During excitation-contraction coupling, depolarization of the cell membrane causes voltage-sensitive L-type Ca^{2+} channels in t-tubules to activate nearby RyRs via either direct physical coupling (in skeletal muscle) (2, 4–6) or an influx of extracellular Ca^{2+} (in cardiac muscle) (2, 4, 7, 8). The latter mechanism is referred to as Ca^{2+}-induced Ca^{2+} release. The massive release of Ca^{2+} from SR by RyRs then initiates a cascade of cellular events that result in muscle contraction.

Outside of striated muscles, all three mammalian RyR isoforms (including the brain isoform/RyR3) are variably expressed in both excitable and non-excitable cells (4, 5, 9–11). In particular, RyRs have been found in various smooth muscle types (12–17), in which the physiological roles and regulatory mechanisms of RyRs are not as well understood as in striated muscles. Previous studies, however, have shown that RyRs in vascular smooth muscle cells may have a role in modulating cerebral and pulmonary arterial blood flow in response to changes in intravascular pressure (18, 19) and oxygen tension (20, 21), respectively. In addition, RyRs in other smooth muscle types may mediate uterine contraction (22, 23) and gastrointestinal tract peristalsis (24–26).

RyRs have also been found in airway smooth muscle cells (ASMCs), in which Ca^{2+} mobilization mediated by RyRs may have a significant role in spasmogen-induced bronchoconstriction (27–30). Airway spasmogens typically induce both Ca^{2+} release from intracellular stores and Ca^{2+} influx in ASMCs (29, 31, 32), which enable Ca^{2+}/calmodulin-dependent myosin light chain kinase to promote cross-bridging of actin and myosin filaments, thereby effecting airway smooth muscle contraction (33). Previous studies have established that many airway spasmogens such as histamine, endothelin, and muscarinic receptor agonists increase the concentration of the second messenger inositol 1,4,5-trisphosphate in ASMCs via activation of G-proteins and phospholipase C (34) The increase in inositol 1,4,5-trisphosphate level subsequently causes stored Ca^{2+} release by IP_3Rs that is followed by store-operated Ca^{2+} influx (1, 29, 32). Analogously, a series of recent studies using airway smooth

* This work was supported by an American Lung Association Grant RG-191-N and an American Heart Association (Mid-Atlantic Affiliate) grant (to J. P. E.) and National Institutes of Health grants (to P. B. R. and G. M.). The costs of publication of this article were defrayed in part by the payment of page charges. This article must therefore be hereby marked "*advertisement*" in accordance with 18 U.S.C. Section 1734 solely to indicate this fact.

‖ To whom correspondence should be addressed: Division of Pulmonary, Allergy and Critical Care Medicine, MSRB 241, Research Dr., Duke University Medical Center, Durham, NC 27710. Tel.: 919-668-3832; Fax: 919-668-0494; E-mail: eu000001@duke.edu.

[1] The abbreviations used are: RyR, ryanodine receptor; ASMC, airway smooth muscle cell; IP_3R, inositol 1,4,5-trisphosphate receptor; SR, sarcoplasmic reticulum; cADPR, cyclic adenosine diphosphate ribose; $[Ca^{2+}]_{cyt}$, cytosolic Ca^{2+} concentration; TRITC, tetramethylrhodamine isothiocyanate; RT, reverse transcription; PBS, phosphate-buffered saline; PIPES, 1,4-piperazinediethanesulfonic acid.

muscles from human, equine, and murine tracheal tissues have suggested that many airway spasmogens such as histamine, bradykinin, and muscarinic receptor agonists also increase the synthesis of the putative RyR agonist cyclic adenosine diphosphate ribose (cADPR) from NAD^+ by cADP-ribosyl cyclase(s) (35–39). In ASMCs, cADPR appears to cause a specific RyR2 accessory protein, FKBP 12.6, to dissociate from RyR2, thereby provoking RyR2 to release stored Ca^{2+} (37). The effect of cADPR on RyR2 may be synergized by the initial increase in cytosolic Ca^{2+} concentration ($[Ca^{2+}]_{cyt}$) (40) mobilized by IP_3Rs and other plasmalemmal Ca^{2+} channels.

Because all three RyR isoforms have been found to be co-expressed in vascular smooth muscle cells (15, 16), we assessed whether RyR isoforms other than RyR2 are expressed in ASMCs and whether these isoforms are also involved in spasmogen-induced bronchoconstriction. Here we report that RyR1 and RyR3 are also expressed in the mouse ASMCs. Our immunofluorescence studies indicate that RyR1 and RyR3 are distributed to different compartments within these cells: RyR1 appears to localize to the periphery near the cell membrane, whereas RyR3 is centrally localized to the perinuclear region. Moreover, our studies of mouse ASMCs and bronchial rings exposed to the prototypic airway spasmogen/muscarinic receptor agonist carbachol indicate that RyR1 and/or RyR3 also mediate the Ca^{2+} response and thus bronchoconstriction as the level of muscarinic receptor stimulation increases. Our findings that suggest different subcellular localizations of RyR isoforms in ASMCs as well as the involvement of multiple RyR isoforms in muscarinic receptor agonist-induced Ca^{2+} response provide new insights into the complex Ca^{2+} signaling in ASMCs.

EXPERIMENTAL PROCEDURES

Materials—Mouse monoclonal anti-RyR1 IgM was obtained from Upstate (Waltham, MA). Mouse monoclonal anti-RyR2 IgG was obtained from Affinity BioReagents (Golden, CO). A rabbit polyclonal IgG raised against a 13-amino acid region specific for RyR3 and a C-terminal cysteine (KKRRRGQKVEKPEC) was prepared as described previously (41). Species-specific fluorescein isothiocyanate-conjugated goat anti-mouse IgM, fluorescein isothiocyanate-conjugated goat anti-mouse IgG, and TRITC-conjugated goat anti-rabbit IgG secondary antibodies were obtained from Jackson ImmunoResearch Laboratories (West Grove, PA). [^{3}H]Ryanodine was obtained from PerkinElmer Life Sciences. Ca^{2+} indicator Fura-2 acetoxymethyl ester was obtained from Molecular Probes (Eugene, OR). Cy3-conjugated mouse monoclonal anti-smooth muscle-specific α-actin IgG, ryanodine, dantrolene, and all other reagents were obtained from Sigma-Aldrich Chemical Co., unless specified otherwise.

Isolation of Mouse Bronchi—Male C57/BL6 mice (age, 11–12 weeks; ~25 g) were obtained from the Jackson Laboratory (Bar Harbor, ME). Each animal was sacrificed after being anesthetized with an intraperitoneal injection of sodium pentobarbital (100 mg/kg). The heart and lungs were then removed *en bloc* and immersed in modified Krebs buffer (118 mM NaCl, 4.8 mM KCl, 1.2 mM $MgSO_4$, 1.2 mM KH_2PO_4, 2.5 mM $CaCl_2$, 25 mM $NaHCO_3$, and 11 mM glucose, pH 7.4), and main bronchi (second generation) and lobar bronchi (third generation) were isolated under microscopic dissection. Adventitial layers were then removed.

Immunoblot Analyses to Detect RyRs in the Mouse Airway and Verify the Specificities of Individual Anti-RyR Antibodies—Second and third generation bronchi from eight mice were pooled and homogenized in a buffer consisting of 320 mM sucrose, 5 mM HEPES, and a protease inhibitor mixture (Complete Mini; Roche Molecular Biochemicals) using a hand-held tissue homogenizer. Microsomal fractions enriched in RyRs were prepared from the homogenate as described previously (42). Twenty μg of microsomal protein samples were separated by 3–8% Tris acetate SDS-PAGE under reducing condition and transferred onto nitrocellulose membranes. The protein concentrations were determined using a Bio-Rad DC protein assay kit. The membranes were first blocked with 5% nonfat milk in 0.05% Tween 20/PBS at 24 °C for 1 h. Following probing with a mouse monoclonal anti-RyR1 IgM (1 ng/μl) or a rabbit polyclonal anti-RyR3 IgG (1:500), the blots were developed using a Vectastain ABC-AmP Western blot detection kit (Vector Laboratories, Burlingame, CA). To verify the specificity of each anti-RyR antibody for the corresponding RyR isoform, tissue homogenates from mouse hind leg skeletal muscle (10 μg/lane), heart (10 μg/lane), and brain (30 μg/lane) that express RyR1, RyR2, and RyR3, respectively (brain also expresses RyR2), were used in a separate immunoblot analysis.

Isolation of Mouse ASMCs—The isolation of second and third generation mouse bronchi was performed as described above, except that modified Krebs buffer and the subsequent buffers used for isolating ASMCs all passed through 0.22 μm Syrfil-MF filters (Whatman) and contained 1% penicillin, 1% streptomycin, and 1% antimycotic antibiotics (Invitrogen). The airways were cut open longitudinally, and the epithelium was rubbed off gently using a cotton tip. The smooth muscle layer was then minced in Ca^{2+}-reduced (20 μM) Hanks' balanced salt solution, followed by digestion in Ca^{2+}-reduced Hanks' balanced salt solution containing 1000 units/ml type II collagenase (Worthington Biochemical Corp., Lakewood, NJ), 10 units/ml papain, 2 mg/ml bovine serum albumin, and 1 mM dithiothreitol for 20 min at 37 °C. The partially digested ASMCs were then centrifuged at 600 × *g* for 1 min, resuspended in Ca^{2+}-free Hanks' balanced salt solution, and gently triturated using a long glass pipette until a large number of elongated cells were observed (43). ASMCs were then centrifuged, collected, and resuspended in M199 media with 10% fetal bovine serum and 1% penicillin/streptomycin. These ASMCs were allowed to grow in the same media over 5–6 days under standard culture conditions before they were detached from the flask with 0.25% trypsin/1.0 mM EDTA for subculture. ASMCs after one or two passages were used in subsequent studies. The homogeneity of ASMCs was assessed using a mouse monoclonal anti-smooth muscle-specific α-actin IgG (see below).

RT-PCR Analyses of RyR Isoforms in Mouse Airways and ASMCs—After removing adventitial tissues, second and third generation bronchi from each animal were pooled and immersed in RNA*later* stabilization solution (Qiagen, Carlsbad, CA) and homogenized using a hand-held tissue homogenizer. In addition, mouse hind leg skeletal muscle, heart, and brain tissues that served as positive control tissues for RyR1, RyR2, and RyR3, respectively, were also homogenized in the same fashion. Total RNA was extracted using the Qiagen RNeasy Midi kit according to the manufacturer's instructions. Similarly, 7–9 day-old cultured mouse ASMCs (~5×10^5) after one or two passages were first detached from culture flasks with 0.25% trypsin/1.0 mM EDTA at room temperature for 5 min, centrifuged at 600 × *g* for 10 min, washed with M199 media twice, and preserved in RNA*later* solution. After homogenization, total RNA was extracted from ASMCs using the Qiagen RNeasy Mini kit. The RT-PCR protocol used to amplify target sequences for each mouse RyR isoform and β-actin that served as internal control was described previously (16). The nucleotide sequences and the lengths of the expected PCR products (in parentheses after each primer pair) for each primer pair were as follows: RyR1, GAAGGTTCTGGACAAACACGGG (forward) and TCGCTCTTGTTGTAGAATTTGCGG (reverse) (435 bp); RyR2, GAATCAGTGAGTTACTGGGCATGG (forward) and CTGGTCTCTGAGTTCTCCAAAAGC (reverse) (658 bp); RyR3, AGAAGAGGCCAAAGCAGAGG (forward) and GGAGGCCAACGGTCAGA (reverse) (269 bp); and β-actin, TGTATGCCTCTGGTCGTACCAC (forward) and ACAGAGTACTTGCGCTCAGGAG (reverse) (592 bp). The RT-PCR products over 35 cycles of amplification were resolved by electrophoresis in 1% agarose gels, visualized on a UV transilluminator, digitally photographed, and analyzed using XCAP software (Epix Inc., Buffalo Grove, IL). The product ratios of target/β-actin were used to assess the relative expression of each RyR isoform mRNA in the mouse airway and in cultured ASMCs.

Immunofluorescence Studies of RyRs in Mouse ASMCs—Primary mouse ASMCs after one passage were cultured in Lab-Tek slide II system (Nalge Nunc International, Naperville, IL) for 7 days. The cells were first washed with PBS (pH 7.4) twice and then fixed with 2% paraformaldehyde in PBS for 15 min at room temperature. After washing with PBS two more times, the remaining paraformaldehyde was then quenched with 0.75% glycine in PBS for 30 min (43). Afterward, the cells were washed with PBS, permeabilized in 0.1% SDS and 0.05% Triton X-100 in PBS for 15 min, blocked with 10% goat serum in PBS for 30 min, and probed with individual antibody specific for each RyR isoform in 1% goat serum/PBS for 1 h. The dilutions for each of these antibodies were 1 ng/μl, 10 ng/μl, and 1:1000 for anti-RyR1, anti-RyR2, and anti-RyR3, respectively. After washing with PBS, cells were incubated with the corresponding fluorochrome-labeled secondary antibody (7.5 ng/μl) in 1% goat serum/PBS for 1 h. Before washing and mounting on Prolong Antifade solution (Molecular Probes), cells were counterstained with 4′,6-diamidino-2-phenylindole, which stained the nuclei. In a few experiments, a goat polyclonal anti-RyR3 antibody (Santa Cruz Biotechnology, Santa Cruz, CA) and TRITC-conjugated donkey anti-

goat IgG were used to confirm the cellular distribution of RyR3 in ASMCs. Each experiment contained at least one control in which only the primary antibody was omitted. The homogeneity of ASMCs was assessed separately in cells that were probed with a Cy3-conjugated mouse monoclonal anti-smooth muscle-specific α-actin IgG and counterstained with 4′,6-diamidino-2-phenylindole. The slides were examined and digitally photographed using an epifluorescent microscope (Olympus BX60) equipped with UPlanFl 20–100× objectives and a mercury lamp.

To assess the relative cellular distribution of RyR1 and RyR3 in mouse ASMCs, in certain studies mouse ASMCs were double-labeled with both mouse monoclonal anti-RyR1 IgM and rabbit polyclonal anti-RyR3 IgG. The prepared slides were examined using the epifluorescent microscope and a Carl Zeiss LSM 510 laser scanning confocal microscopy system attached to an Axiovert 100 inverted microscope (Carl Zeiss, Jena, Germany). Argon and helium/neon lasers provided the excitation light beams (488 and 543 nm, respectively) for the confocal microscopy system. The green (fluorescein isothiocyanate) and orange (TRITC) emissions were filtered (515–540- and 585–615-nm bandpass filters, respectively), and images (512 × 512 pixels) obtained with a 63× objective (Plan-Neofluar) were recorded using LSM Image software.

Carbachol-induced Contractile Responses of Isolated Mouse Bronchial Rings—Four bronchial rings (inner diameter, ~0.5 mm; length, ~2 mm) cut from second and third generation bronchi from each mouse were studied in parallel. Each bronchial ring was mounted horizontally on two tungsten triangles (diameter of tungsten wire, ~100 μm) and submerged in Krebs buffer in a thermostatted organ bath constantly bubbled with a pre-mixed gas consisting of 20% O_2, 5% CO_2 and balance N_2 (44). The temperature in the organ bath was maintained at 37 °C. The two tungsten triangles (and thus the bronchial ring) were suspended between a stainless steel wire hook connected to a Grass FT-03 force displacement transducer (West Warwick, RI) and a glass hook inside the organ bath that served as an anchor. An optimal resting tension of 0.3 g was applied to each ring during the initial equilibration period of 30 min. The bronchial rings were then constricted stepwise with 50 and 80 mM KCl (final concentration) over 20 min to determine the viability of bronchial rings and establish references for comparison. Approximately 30 min after removing excess KCl, bronchial rings were treated stepwise with 10 nM to 3 μM cumulative doses of carbachol (>3 μM carbachol did not produce higher contractile responses) at 5–8-min intervals that allowed the contractile responses (isometric tensions) of bronchial rings after each carbachol challenge to reach steady state. In specified experiments, an inhibitor of RyRs (ryanodine dissolved in Krebs buffer or dantrolene dissolved in Me_2SO) was added to the organ bath 20 min before the stepwise addition of carbachol. In a typical study, two of the bronchial rings were pre-treated with a RyR inhibitor, whereas the other two rings that served as concurrent controls were pre-treated with equal volumes of delivery vehicle. Increases in isometric tension were amplified (Grass DC pre/amplifier model 7DAF) and recorded digitally (Polyview software; Grass-Telefactor). The increases in steady-state isometric tension of mouse bronchial rings caused by cumulative doses of carbachol were normalized against individual ring increases in isometric tensions generated by 80 mM KCl (higher concentrations of KCl did not cause further constriction in mouse bronchial rings).

Carbachol-induced Calcium Responses of Mouse ASMCs—Mouse ASMCs after one or two passages in M199 media containing 10% fetal bovine serum were grown over ~7 days in a culture coverslip/dish (MatTek, Ashland, MA) designed for live cell imaging. Mouse ASMCs were first loaded with 5 μM Fura-2 acetoxymethyl ester in M199 media containing 10% fetal bovine serum for 30 min and then washed with HEPES-buffered Tyrode solution (145 mM NaCl, 2.8 mM KCl, 2 mM $MgSO_4$, 2 mM $CaCl_2$, 10 mM HEPES, and 10 mM glucose, pH 7.4) three times to remove excess Ca^{2+} indicator. The culture dish was then placed onto a stage mounted on an inverted microscope (Nikon Eclipse TE2000). After pre-treatment with 200 μM ryanodine, 25 μM dantrolene, or the delivery vehicle for 5 min, increased doses of carbachol (10 nM to 10 μM, cumulative concentrations) were introduced to ASMCs stepwise at 5–7-min intervals. Fluorescence measurements were performed under ambient temperature (21 °C) on small groups of dispersed, elongated cells viewed with a Nikon UV-Fluor 40× oil immersion objective (~4–5 cells were studied in each experiment). These ASMCs were excited alternatively at 340 and 380 nm using a Lambda DG4 filtering system (Sutter Instruments) that provided rapid excitation filter changes. Illumination was provided by a xenon arc lamp. Emitted fluorescence was filtered by a 490–530-nm bandpass filter and captured on a Cool SNAP HQ charge-coupled device camera. Video images were digitized onto a computer and analyzed using MetaMorph/MetaFluor software (Universal Imaging Corp.). Ratiometric Ca^{2+} images were generated at 1-s intervals. For each cell, Ca^{2+} responses to stepwise carbachol challenges were reflected as a change in fluorescence ratio (F_{340}/F_{380}) of Fura-2 at steady-state averaged from pixels within cytoplasmic areas (45). In control experiments without cells, neither 200 μM ryanodine nor 25 μM dantrolene had any noticeable effect on F_{340}/F_{380} of Fura-2.

Isoform Specificity of the RyR Inhibitor Dantrolene—[^{3}H]Ryanodine binding to RyRs, which correlates non-linearly with RyR channel activities (46, 47), was used to assess the effect of dantrolene on each RyR isoform. Rabbit skeletal muscle and canine cardiac SR vesicles that served as sources of RyR1 and RyR2 were isolated as previously described (46, 48). To obtain RyR3 for this study, crude microsomal fractions from HEK cells containing heterologously expressed rabbit RyR3 were prepared as previously described (49).

Unless otherwise indicated, cardiac muscle, skeletal muscle SR vesicles (0.2 mg/ml), or microsomal fractions from HEK cells containing the heterologously expressed RyR3 (0.4 mg/ml) were exposed to various concentrations of dantrolene (0–50 μM) and incubated for 2 h at 37 °C with 5 nM [^{3}H]ryanodine in media containing 150 mM KCl, 20 mM imidazole, pH 7.0, 0.3 mM Pefabloc, 30 μM leupeptin, 2 mM adenylyl 5′-(β,γ-methylene)diphosphonate, 1.5 mM Mg^{2+}, 1 μM calmodulin, and 0.3–0.4 μM free Ca^{2+}. Nonspecific binding was determined using a 1000-fold excess of unlabeled ryanodine. Aliquots of the samples were diluted with 20 volumes of ice-cold water and placed on Whatman GF/B filters soaked with 2% (w/w) polyethyleneimine. Filters were washed with three 5-ml volumes of ice-cold 100 mM KCl, 1 mM PIPES (pH 7) buffer, and the radioactivity remaining on the filters was determined by liquid scintillation counting to obtain bound [^{3}H]ryanodine (46).

Data Analysis—All results are expressed as means ± S.E. Significance of differences of data was analyzed with Student's t test. A p value of <0.05 was considered statistically significant.

RESULTS

Detection of RyR Isoforms in the Mouse Airway and ASMCs—In immunoblot studies, RyR1 and RyR3 were detected in the microsomal fractions isolated from mouse bronchi (Fig. 1*A*). We also detected RyR2 in immunoblots using a RyR2-specific antibody; however, no immunofluorescence was detected in the localization studies (data not shown). The isoform specificity of anti-RyR1 and anti-RyR3 antibodies was confirmed using positive control tissues (Fig. 1*B*). Each of these RyR-isoform specific antibodies appears to recognize only the corresponding RyR isoform. The identification of all three RyR isoforms in the mouse bronchi was corroborated by RT-PCR analyses (Fig. 1*C*). Because the airway contains other cell types that may express RyRs (50), we examined whether all three RyR isoforms are expressed within mouse ASMCs. In cultured ASMCs, all stained positive for smooth muscle-specific α-actin (Fig. 2*A*), and mRNAs for all three RyR isoforms were also detected by RT-PCR (Fig. 1*C*). Although RyR2 appears to be the most abundantly expressed RyR isoform in mouse bronchi by RT-PCR (using β-actin as internal controls), RyR1 is more abundantly expressed in cultured ASMCs than RyR2 and RyR3 (Fig. 1*D*).

Subcellular Localization of RyR Isoforms in Mouse ASMCs—To assess the subcellular localization of RyR isoforms, cultured mouse ASMCs were probed with individual isoform-specific anti-RyR antibodies used in our immunoblot studies. As shown in Fig. 2, in mouse ASMCs, RyR1 is distributed more peripherally in close proximity to the cell membrane, whereas RyR3 is distributed more centrally around the nucleus. The perinuclear distribution of RyR3 in mouse ASMCs was also found in limited experiments using a different goat polyclonal anti-RyR3 IgG (Santa Cruz Biotechnology; data not shown). Although the expression of RyR2 in mouse ASMCs is demonstrated by RT-PCR (Fig. 1, *C* and *D*), RyR2 was not detected in mouse ASMCs by the immunofluorescence method (data not shown), possibly due to a lack of efficacy of this particular antibody in immunohistochemical studies. Because no other RyR2-specific antibody is currently available, the distribution of RyR2 in ASMCs remains undefined.

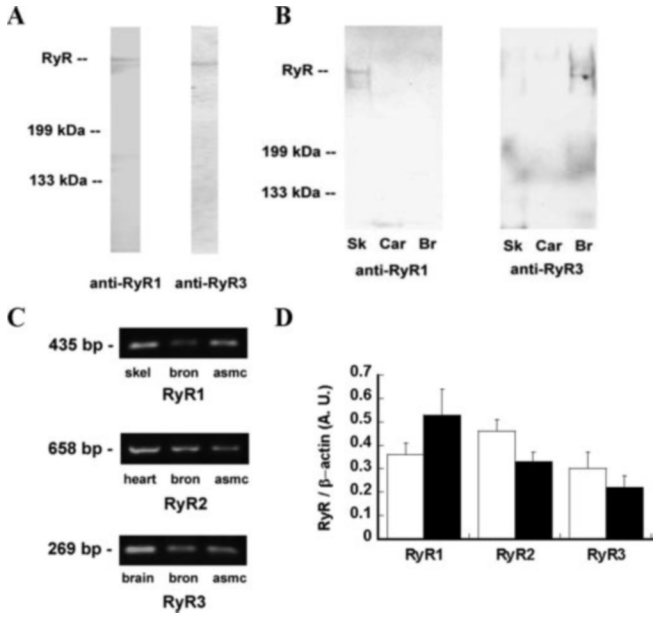

FIG. 1. **Expression of RyR isoforms in mouse bronchi and cultured ASMCs.** *A*, immunoblot studies using anti-RyR1 and anti-RyR3 antibodies indicate that RyR1 and RyR3 are present in the microsomal fractions isolated from mouse bronchi. *B*, immunoblot analyses of homogenates from skeletal muscle (*Sk*), heart (*Car*), and brain (*Br*) that express RyR1, RyR2, and RyR3, respectively, show the isoform specificities of anti-RyR1 and anti-RyR3 antibodies. *C*, RT-PCR analyses using isoform-specific primers labeled at the bottom show the expression of three RyR isoforms in mouse bronchi (*bron*). Mouse skeletal muscle (*skel*), heart, and brain were used as positive control tissues for RyR1, RyR2, and RyR3, respectively. All RyR isoforms are also detected in cultured mouse ASMCs (Fig. 2*A*) by RT-PCR. *D*, semiquantitative analysis of individual RyR isoform expression in mouse bronchi (□) and in cultured ASMCs (■) using β-actin as internal controls ($n = 3$ independent experiments).

Ca^{2+} Mobilization by RyRs in Mouse Airway Smooth Muscle Provoked by Carbachol—We used two complementary methods to assess the extent that RyRs contribute to Ca^{2+} mobilization in ASMCs provoked by the prototypic airway spasmogen/muscarinic receptor agonist carbachol. We first determined the carbachol-induced contractile responses of mouse bronchial rings in the presence or absence of inhibitory concentrations of ryanodine, which inhibits all three RyR isoforms, but not other Ca^{2+} channels such as IP_3Rs (4, 51). Stepwise additions of 10 nM to 3 μM carbachol (cumulative concentrations) caused isolated bronchial rings to develop graded increases in isometric tension that reached steady state ~5 min after each carbachol challenge (Fig. 3*A*). The contractile effects of carbachol first became prominent at 100 nM and reached maximum at ~2 μM. In comparison to their concurrent controls, bronchial rings pre-treated with 200 or 300 μM ryanodine developed significantly less contractile response to each corresponding dose of carbachol (Fig. 3, *A* and *B*). In complementary studies of cultured mouse ASMCs, the graded Ca^{2+} responses of these cells to stepwise carbachol challenges, as reflected by the increases in F_{340}/F_{380} ratio of Ca^{2+} indicator Fura-2 at steady state, were also significantly suppressed by 200 μM ryanodine throughout the entire range of carbachol used (Fig. 3*C*). Thus, the inhibitory effects of ryanodine on bronchial rings challenged with carbachol are due to a decrease in Ca^{2+} mobilization by RyRs in ASMCs.

Inhibition of RyR1 and RyR3 Suppressed the Responses of Bronchial Rings and ASMCs to High but Not Low Doses of Carbachol—Our studies of mouse ASMCs and bronchial rings in the presence or absence of inhibitory concentrations of ryanodine (Fig. 3) indicate that Ca^{2+} mobilization by RyRs contributes to muscarinic receptor-mediated bronchoconstriction in mice as in other animal species (27, 37). Because a previous study using equine tracheal smooth muscle has implicated RyR2 in this process (37), but we have also identified RyR1 and RyR3 in the mouse airway smooth muscle (Figs. 1 and 2), we used dantrolene, an inhibitor of RyR1 and RyR3, but not of RyR2 (47), to determine whether RyR1 and/or RyR3 may also play a role in carbachol-induced responses of mouse ASMCs and bronchial rings. We first used an indirect assay of RyR channel activity, the [^{3}H]ryanodine binding assay (46), to confirm the reported effects of dantrolene on individual RyR isoforms (47) as well as to determine the optimal concentrations of dantrolene in the subsequent mouse ASMCs and bronchial ring studies (Fig. 4*A*). The amounts of [^{3}H]ryanodine bound to skeletal muscle and cardiac muscle SR preparations at steady state correlate non-linearly with the channel activities of RyR1 and RyR2, respectively (40, 46). Because purifying RyR3 from native tissues is confounded by the co-expression of other RyR isoforms in those tissues, microsomal fractions from HEK cells heterologously expressing only RyR3 were used in this study. As shown in Fig. 4*A*, dantrolene suppressed the channel activities of RyR1 and RyR3 under our *in vitro* experimental conditions, although the effect of dantrolene on RyR3 was only modest. The suppressive effects of dantrolene on RyR1 and RyR3 plateaued at ~15 μM. In contrast, RyR2 appears to be insensitive to dantrolene up to 50 μM.

The effects of dantrolene on carbachol-induced contractions of mouse bronchial rings were then assessed. To ensure tissue penetration of dantrolene that would maximally inhibit RyR1 and RyR3 but not cause untoward effects (Fig. 4*A*), 25 μM dantrolene was used in these experiments. Unlike the non-isoform-specific RyR inhibitor ryanodine (Fig. 3, *A* and *B*), 25 μM dantrolene had no significant inhibitory effect on the contractile responses of mouse bronchial rings challenged with 50–500 nM carbachol (Fig. 4, *B* and *C*; 50 μM dantrolene also failed to suppress the contractile responses of 50–500 nM carbachol, data not shown). At higher doses of carbachol, however, the suppressive effects of 25 μM dantrolene on mouse bronchial rings were comparable to those of 200 or 300 μM ryanodine (Fig. 3*B*). Analogously, as compared with the control group, mouse ASMCs pre-treated with 25 μM dantrolene had smaller Ca^{2+} responses only at carbachol concentrations of >500 nM (Fig. 4*D*). Because dantrolene inhibits the responses of ASMCs and bronchial rings only when the cumulative doses of carbachol were >500 nM, RyR1 and/or RyR3 appear to contribute to the Ca^{2+} mobilization in ASMCs when the level of muscarinic receptor stimulation is high.

DISCUSSION

Although previous studies using pharmacological agents have consistently suggested the presence of functional RyRs in ASMCs from various mammalian species (27, 35, 37, 51), relatively little is known about the expression and physiological roles of individual RyR isoforms in this type of smooth muscle. Using RT-PCR, one study identified RyR3 exclusively in human bronchial ASMCs (51), whereas other studies had found RyR2 to be the predominant RyR isoform in tracheal smooth muscle cells using RT-PCR and immunoblot analyses (17, 37) (low expression of RyR1 and RyR3 was also detected by RT-PCR (17)). In contrast, our studies indicate that all three RyR forms are comparably expressed in the mouse airway and in primary cultured ASMCs (Fig. 1). The co-expression of all three RyR isoforms in a single smooth muscle cell type has also been described in various types of murine vascular smooth muscle cells (14, 16). The discrepancy of RyR expression in ASMCs between this study and previous studies could be due to a difference in techniques used and/or variations among different

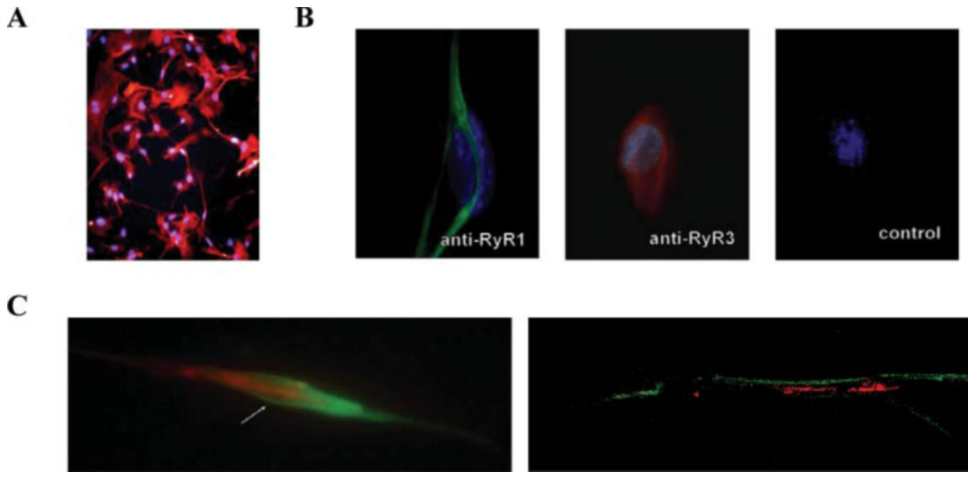

FIG. 2. **Subcellular localization of RyR isoforms in mouse ASMCs.** *A*, the purity of mouse ASMCs was assessed using a Cy3-conjugated mouse monoclonal anti-smooth muscle-specific α-actin IgG that stained the cytoplasm of ASMCs *orange*. *B*, mouse ASMCs were probed with anti-RyR1 or anti-RyR3 antibody as indicated. Control was probed with a combination of fluorescent secondary antibodies. Nuclei are stained *blue* with 4′,6-diamidino-2-phenylindole stain. *C*, an epifluorescence image of a mouse ASMC double-labeled with mouse monoclonal anti-RyR1 IgM and rabbit polyclonal anti-RyR3 IgG (*left panel*) also suggests the peripheral distribution (*arrow*) of RyR1 (*green*) and the perinuclear distribution of RyR3 (*orange*). A confocal microscopy image (*right panel*) of a similarly labeled ASMC (optical slice, 0.5 μm).

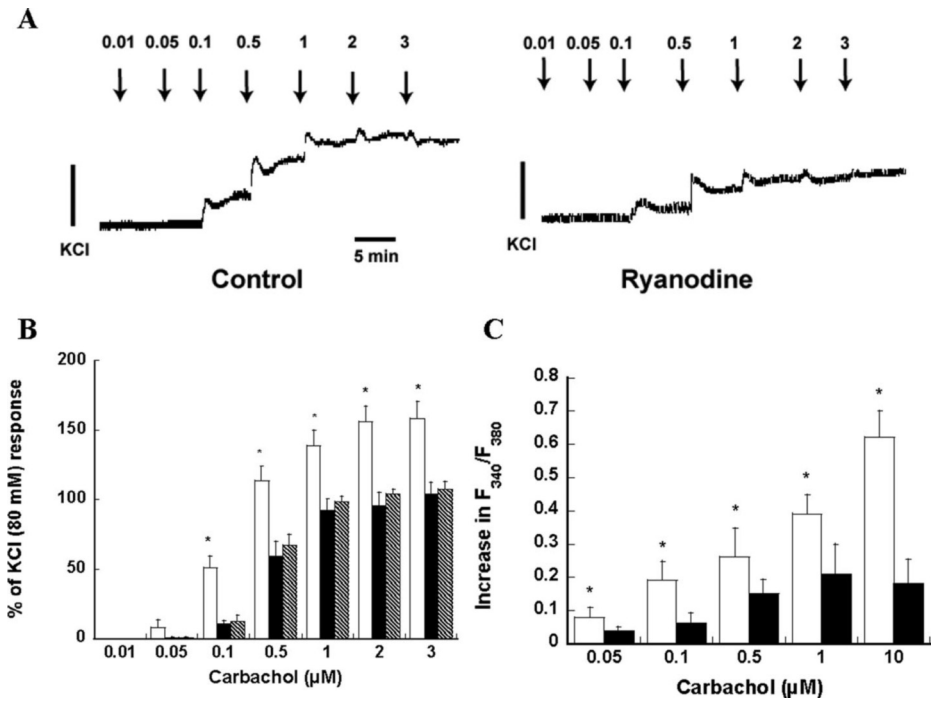

FIG. 3. **Effects of ryanodine on carbachol-induced contractile responses of mouse bronchial rings and Ca^{2+} responses of ASMCs.** *A*, representative traces of mouse bronchial rings responding to increased doses of carbachol without (*left panel*) or with (*right panel*) pretreatment with ryanodine. Increased doses of carbachol (cumulative concentrations, in μM) were added to the organ baths as indicated (*arrows*). *Vertical bars* indicate the contractile responses of individual bronchial rings to 80 mM KCl obtained prior to the addition of ryanodine and carbachol. *B*, the increases in steady-state isometric tension of mouse bronchial rings (normalized to 80 mM KCl response) caused by 10 nM to 3 μM carbachol were significantly attenuated by pre-treatment with 200 μM ryanodine (*black bars*, $n = 10$) or 300 μM ryanodine (*shaded bars*, $n = 6$) as compared with concurrent controls (*white bars*, $n = 14$). *, $p < 0.01$ *versus* groups pre-treated with ryanodine. *C*, Ca^{2+} responses of mouse ASMCs at steady state, as reflected by the changes in the fluorescence ratio (F_{340}/F_{380}) of Ca^{2+} indicator Fura-2, to increased doses of carbachol (50 nM to 10 μM, cumulative concentrations) in the presence (■; $n = 13$ cells) or absence (□; $n = 15$ cells) of 200 μM ryanodine. *, $p < 0.01$ *versus* 200 μM ryanodine group.

mammalian species studied. To detect the relatively low concentrations of RyRs in the airway, we used microsomal preparations enriched in RyRs (42) isolated from mouse bronchi in our immunoblot studies. Our studies of rat airways using RT-PCR and immunoblot analyses also indicate that all three RyR isoforms are expressed in rat bronchi,[2] thus it appears that all three RyR isoforms are expressed in the murine airway.

More importantly, the results from our studies of mouse ASMCs and bronchial rings add to an emerging body of data that supports a significant role for RyRs in Ca^{2+} signaling in various smooth muscle types (16, 21, 25, 30). These data may eventually modify the prevailing view that IP_3Rs are the main intracellular Ca^{2+} release channel family mediating Ca^{2+} signaling in smooth muscle cells in response to external stimuli. As in the case of muscarinic receptor-mediated bronchoconstriction, the type of airway constriction most extensively studied as well as the most relevant (52, 53), stored Ca^{2+} release by IP_3Rs has long been thought to be the dominant cellular process that results in an increase in $[Ca^{2+}]_{cyt}$ and thus bronchoconstriction (34, 54, 55). Our data as well as results of other groups (30, 35–37), however, suggest that RyRs also contribute significantly to the overall Ca^{2+} responses of ASMCs stimulated with muscarinic receptor agonists. Depending on the dose of carbachol, inhibiting RyRs but not IP_3Rs with ryanodine suppressed ~40–60% of carbachol-induced responses of ASMCs and bronchial rings (Fig. 3). The roles of IP_3Rs and RyRs in airway spasmogen-induced Ca^{2+} mobilization, however, need not be mutually exclusive: because RyRs are sensitive to Ca^{2+} activation (*i.e.* Ca^{2+}-induced Ca^{2+} release) (4, 5), Ca^{2+} mobilization mediated by RyRs in spasmogen-provoked ASMCs may be a downstream signaling event after the initial Ca^{2+} release by IP_3Rs (30, 37). In the case of RyR2 in ASMCs,

[2] W. Du and J. P. Eu, unpublished data.

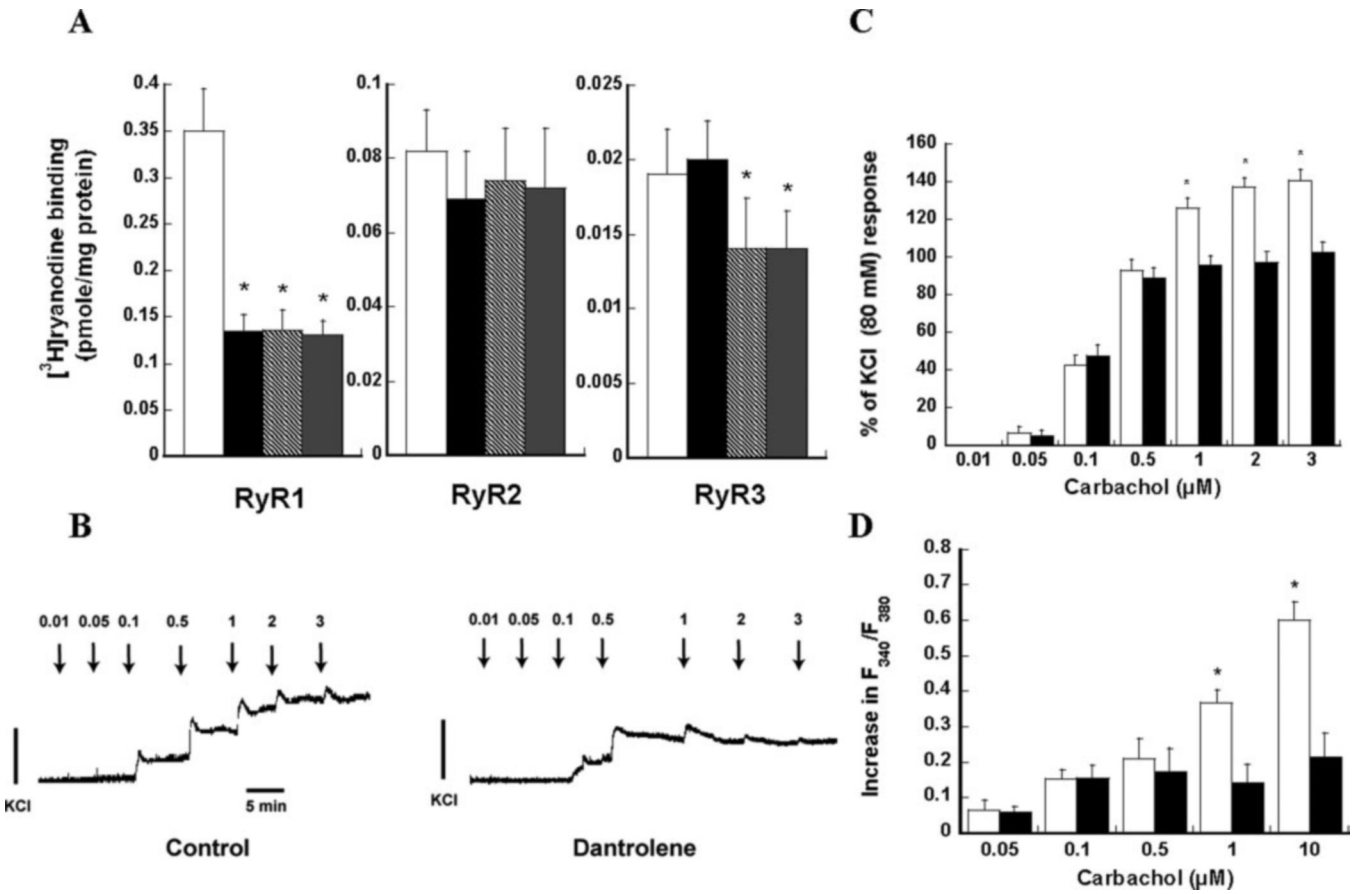

FIG. 4. **Specificity of dantrolene and its effects on carbachol-induced responses of mouse bronchial rings and ASMCs.** *A*, effects of different concentrations of dantrolene (*white bars*, control; *black bars*, 1 μM; *shaded bars*, 15 μM; and *dark gray bars*, 50 μM; $n = 4–7$ experiments) on [^{3}H]ryanodine binding to the indicated individual RyR isoform were determined as described under "Experimental Procedures." *, $p < 0.05$ *versus* control group. *B*, typical traces of mouse bronchial rings responding to increased doses of carbachol after pre-treatment with 25 μM dantrolene (*right panel*) or with an equal volume of delivery vehicle (Me_2SO). *Vertical bars* indicate the contractile responses of individual bronchial rings to 80 mM KCl. *C*, as compared with concurrent controls (*white bars*, $n = 20$), the steady-state isometric tensions of mouse bronchial rings pre-treated with 25 μM dantrolene (*black bars*, $n = 19$) are significantly lower only when the cumulative concentrations of carbachol are >500 nM. *, $p < 0.01$ *versus* 25 μM dantrolene groups. *D*, graded Ca^{2+} responses of mouse ASMCs to a range of carbachol (50 nM to 10 μM) pre-treated with 25 μM dantrolene (*black bars*, $n = 14$) or delivery vehicle (*white bars*, $n = 18$). *, $p < 0.01$ *versus* 25 μM dantrolene group.

this process may be further assisted by an increase in synthesis of the putative endogenous RyR2 agonist cADPR (37) following muscarinic receptor stimulation (Fig. 5). The signaling pathways by which individual RyR isoforms are activated in ASMCs stimulated with spasmogens will require additional studies.

Our immunofluorescence studies of RyR isoforms provide additional insights into the complex Ca^{2+} signaling in ASMCs. Although we were unable to determine the subcellular localization of RyR2 in ASMCs, our results demonstrate for the first time the different subcellular localizations of RyR1 and RyR3 in ASMCs (and to our knowledge, for the first time in any smooth muscle cell type). RyR1 in ASMCs appears to be distributed peripherally near the cell membrane, whereas RyR3 is distributed more centrally around the nucleus (Fig. 2). Our findings complement the results of an immunoelectron microscopy study that showed RyRs are distinctly localized to both central and peripheral SR elements in vas deferens smooth muscle cells (14). Thus, the distinct subcellular localizations of different RyR isoforms as seen in ASMCs could also be present in other smooth muscle cell types.

The peripheral distribution of RyR1 in ASMCs suggests potential functional couplings between RyR1 and other plasmalemmal Ca^{2+} channels in mediating Ca^{2+} mobilization: 1) RyR1 could release stored Ca^{2+} in response to an activation of voltage-sensitive L-type Ca^{2+} channels (4); 2) the potential proximity of RyR1 and other plasmalemmal Ca^{2+} channels raises

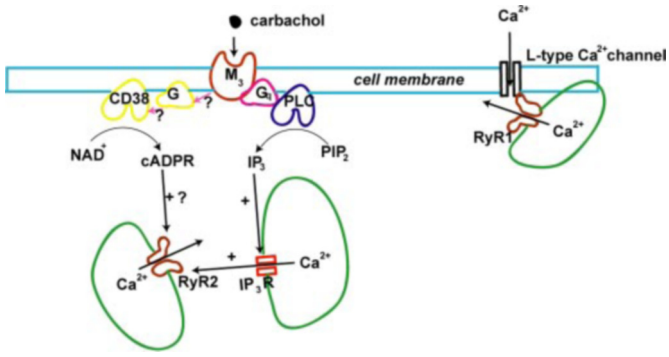

FIG. 5. **Potential pathways of Ca^{2+} mobilization mediated by RyRs in ASMCs following muscarinic receptor stimulation.** RyRs, including RyR3 (which is not shown), may be activated by an initial increase in $[Ca^{2+}]_{cyt}$ (from stored Ca^{2+} release via the G-protein-phospholipase C-IP_3R pathway or Ca^{2+} influx via plasmalemmal Ca^{2+} channels) following the binding of an agonist (carbachol) to the type 3 muscarinic receptors (M_3) of ASMCs (54). RyR2 may be activated first in ASMCs because it is most sensitive to Ca^{2+}-induced Ca^{2+} release. In addition, muscarinic receptor agonists can also causes cADP-ribosyl cyclase(s) such as CD38 (39) to covert NAD^+ to cADPR, which then provokes RyR2 (37) to release stored Ca^{2+}. Because RyR1 is localized to the periphery of ASMCs, RyR1 may be functionally coupled to plasmalemmal ion channels such as L-type Ca^{2+} channels. A "bi-directional signaling" between the two Ca^{2+} channels may promote both Ca^{2+} release by RyR1 and Ca^{2+} influx via the L-type Ca^{2+} channel as has been described in skeletal muscle (56).

the possibility of a retrograde activation of the L-type Ca^{2+} channels by RyR, as has been found in skeletal myocytes (56) and neurons (57); and 3) RyR1 could also be involved in stored-operated Ca^{2+} influx induced by the depletion of RyR-gated intracellular Ca^{2+} stores of ASMCs (29). In addition, in other smooth muscle cell types such as rat cerebral arterial smooth muscle cells, localized Ca^{2+} release by RyRs known as Ca^{2+} sparks can modulate other Ca^{2+}-sensitive plasmalemmal ion channels such as Cl^- or large conductance K^+ channels, thereby altering cell membrane potential and Ca^{2+} influx via voltage-sensitive L-type Ca^{2+} channels (18, 19). Inhibition of RyR1 in this scenario, however, should enhance rather than suppress Ca^{2+} mobilization. This is not supported by our studies using dantrolene (Fig. 4, *B*–*D*). We have attempted to determine the importance of Ca^{2+} influx in Ca^{2+} mobilization mediated by RyRs. However, both mouse ASMCs and isolated bronchial rings quickly lost their carbachol-induced responses in the absence of extracellular Ca^{2+} (data not shown). Thus, to determine whether Ca^{2+} mobilization mediated by RyR1 in mouse ASMCs involves Ca^{2+} influx will require direct measurements of membrane potential and Ca^{2+} currents across the cell membrane.

The results of our studies using dantrolene, which has no inhibitory effect on RyR2 (47) (also see Fig. 4*A*), suggest that Ca^{2+} mobilization and thus bronchoconstriction mediated by RyR1 and/or RyR3 in the mouse airway smooth muscle become more prominent as the intensity of muscarinic receptor stimulation increases (Fig. 4, *B*–*D*). Because a previous study of human airway smooth muscle that expressed RyR3 exclusively did not find a role for RyR in muscarinic receptor-mediated responses (51), RyR1 could be the main RyR isoform contributing to the Ca^{2+} mobilization in ASMCs as the intensity of muscarinic receptor stimulation increases. Because mice deficient in RyR3 are viable, unlike their counterparts deficient in RyR1 or RyR2, this possibility could be tested in future studies.

Because dantrolene, unlike ryanodine, did not inhibit the carbachol-induced responses of ASMCs and bronchial rings at lower doses of carbachol (Fig. 4, *B* and *C*), RyR2 could be the RyR isoform that mobilizes Ca^{2+} in ASMCs provoked by low concentrations of muscarinic receptor agonists. One possibility for this observation is that RyR2 is the RyR isoform most sensitive to Ca^{2+}-induced Ca^{2+} release (4). Thus, RyR1 and/or RyR3 are only activated as the higher intensity of muscarinic receptor stimulation causes further increases in $[Ca^{2+}]_{cyt}$. The other possibility is that only RyR2 is sensitive to the putative endogenous RyR2 agonist cADPR, whose synthesis is increased in spasmogen-provoked ASMCs (37) (Fig. 5). The latter explanation is supported by a recent study that found, when compared with the Ca^{2+} responses of ASMCs from wild-type mice, the Ca^{2+} responses of ASMCs from mice lacking an enzyme critical for synthesis of cADPR in the airway were more attenuated when muscarinic receptor stimulation was relatively low (39). Additional experiments will be needed to study the potential sequential activations of different RyR isoforms in ASMCs. However, because neither RyR2-specific inhibitors nor RyR2-deficient mice are available, further understanding of distinct roles of individual RyR isoforms in ASMCs as well as in other smooth muscle cell types will likely require using gene-silencing techniques. The gene-silencing approach may also be used to study subcellular Ca^{2+} signaling mediated by RyR1 and RyR3 in ASMCs because there is no inhibitor that selectively inhibits RyR1 or RyR3.

Our studies of RyR isoforms in mouse ASMCs provide new insight into the complex Ca^{2+} signaling in these cells. In addition to the ensemble of Ca^{2+} channels that have already been shown to mediate the contractile responses of airways (32, 54, 58), our data, along with results from other groups, suggest that Ca^{2+} mobilization by RyRs is also important in bronchoconstriction. RyRs thus may be exploited as therapeutic targets in respiratory disorders characterized by excessive bronchoconstriction.

Acknowledgments—We thank Kelly Evans and Dan A. Pasek for performing the [^{3}H]ryanodine binding assays and Dr. F. Guilak for help with confocal microscopy. We also thank Drs. Timothy J. McMahon and Rajesh Bhagat for helpful comments.

REFERENCES

1. Berridge, M. J. (1993) *Nature* **361,** 315–325
2. Meissner, G. (1994) *Annu. Rev. Physiol.* **56,** 485–508
3. Lai, F. A., Erickson, H. P., Rousseau, E., Liu, Q. Y., and Meissner, G. (1988) *Nature* **331,** 315–319
4. Franzini-Armstrong, C., and Protasi, F. (1997) *Physiol. Rev.* **77,** 699–729
5. Fill, M., and Copello, J. A. (2002) *Physiol. Rev.* **82,** 893–922
6. Tanabe, T., Beam, K. G., Adams, B. A., Niidome, T., and Numa, S. (1990) *Nature* **346,** 567–569
7. Franzini-Armstrong, C., Protasi, F., and Ramesh, V. (1998) *Ann. N. Y. Acad. Sci.* **853,** 20–30
8. Protasi, F., Franzini-Armstrong, C., and Allen, P. D. (1998) *J. Cell Biol.* **140,** 831–842
9. Ogawa, Y., Kurebayashi, N., and Murayama, T. (1999) *Adv. Biophys..* **36,** 27–64
10. Sutko, J. L., and Airey, J. A. (1996) *Physiol. Rev.* **76,** 1027–1071
11. Ledbetter, M. W., Preiner, J. K., Louis, C. F., and Mickelson, J. R. (1994) *J. Biol. Chem.* **269,** 31544–31551
12. Xu, L., Lai, F. A., Cohn, A., Etter, E., Guerrero, A., Fay, F. S., and Meissner, G. (1994) *Proc. Natl. Acad. Sci. U. S. A.* **91,** 3294–3298
13. Katsuyama, H., Ito, S., Itoh, T., and Kuriyama, H. (1991) *Pflugers Arch.* **419,** 460–466
14. Lesh, R. E., Nixon, G. F., Fleischer, S., Airey, J. A., Somlyo, A. P., and Somlyo, A. V. (1998) *Circ. Res.* **82,** 175–185
15. Neylon, C. B., Richards, S. M., Larsen, M. A., Agrotis, A., and Bobik, A. (1995) *Biochem. Biophys. Res. Commun.* **215,** 814–821
16. Coussin, F., Macrez, N., Morel, J. L., and Mironneau, J. (2000) *J. Biol. Chem.* **275,** 9596–9603
17. Kannan, M. S., Prakash, Y. S., Brenner, T., Mickelson, J. R., and Sieck, G. C. (1997) *Am. J. Physiol.* **272,** Pt 1, L659—L664
18. Brenner, R., Perez, G. J., Bonev, A. D., Eckman, D. M., Kosek, J. C., Wiler, S. W., Patterson, A. J., Nelson, M. T., and Aldrich, R. W. (2000) *Nature* **407,** 870–876
19. Jaggar, J. H., Wellman, G. C., Heppner, T. J., Porter, V. A., Perez, G. J., Gollasch, M., Kleppisch, T., Rubart, M., Stevenson, A. S., Lederer, W. J., Knot, H. J., Bonev, A. D., and Nelson, M. T. (1998) *Acta Physiol. Scand.* **164,** 577–587
20. Gelband, C. H., and Gelband, H. (1997) *Circulation* **96,** 3647–3654
21. Jabr, R. I., Toland, H., Gelband, C. H., Wang, X. X., and Hume, J. R. (1997) *Br. J. Pharmacol.* **122,** 21–30
22. Barata, H., Thompson, M., Zielinska, W., Han, Y. S., Mantilla, C. B., Prakash, Y. S., Feitoza, S., Sieck, G., and Chini, E. N. (2004) *Endocrinology* **145,** 881–889
23. Martin, C., Chapman, K. E., Thornton, S., and Ashley, R. H. (1999) *Biochim. Biophys. Acta* **1451,** 343–352
24. Kuemmerle, J. F., and Makhlouf, G. M. (1995) *J. Biol. Chem.* **270,** 25488–25494
25. Kuemmerle, J. F., Murthy, K. S., and Makhlouf, G. M. (1998) *Cell Biochem. Biophys.* **28,** 31–44
26. Sato, K., Sanders, K. M., Gerthoffer, W. T., and Publicover, N. G. (1994) *Am. J. Physiol.* **267,** Pt 1, C1666–C1673
27. Sieck, G. C., Kannan, M. S., and Prakash, Y. S. (1997) *Can. J. Physiol. Pharmacol.* **75,** 878–888
28. Amrani, Y., Tliba, O., Deshpande, D. A., Walseth, T. F., Kannan, M. S., and Panettieri, R. A., Jr. (2004) *Curr. Opin. Pharmacol.* **4,** 230–234
29. Ay, B., Prakash, Y. S., Pabelick, C. M., and Sieck, G. C. (2004) *Am. J. Physiol. Lung Cell Mol. Physiol.* **286,** L909–L917
30. Bergner, A., and Sanderson, M. J. (2002) *J. Gen. Physiol.* **119,** 187–198
31. Kotlikoff, M. I., Kume, H., and Tomasic, M. (1992) *Biochem. Pharmacol.* **43,** 5–10
32. Sweeney, M., McDaniel, S. S., Platoshyn, O., Zhang, S., Yu, Y., Lapp, B. R., Zhao, Y., Thistlethwaite, P. A., and Yuan, J. X. (2002) *J. Appl. Physiol.* **92,** 1594–1602
33. de Lanerolle, P., and Paul, R. J. (1991) *Am. J. Physiol.* **261,** Pt 1, L1–L14
34. Janssen, L. J., and Daniel, E. E. (1997) in *The Lung: Scientific Foundations* (Crystal, R. G., West, J. B., Weibel, E. R., and Barnes, P. J., eds) pp. 1235–1267, Lippincott-Raven, Philadelphia
35. Deshpande, D. A., Dogan, S., Walseth, T. F., Miller, S. M., Amrani, Y., Panettieri, R. A., and Kannan, M. S. (2004) *Am. J. Respir. Cell Mol. Biol.* **31,** 36–42
36. Deshpande, D. A., Walseth, T. F., Panettieri, R. A., and Kannan, M. S. (2003) *FASEB J.* **17,** 452–454
37. Wang, Y. X., Zheng, Y. M., Mei, Q. B., Wang, Q. S., Collier, M. L., Fleischer, S., Xin, H. B., and Kotlikoff, M. I. (2004) *Am. J. Physiol. Cell Physiol.* **286,** C538–C546
38. Prakash, Y. S., Kannan, M. S., Walseth, T. F., and Sieck, G. C. (1998) *Am. J. Physiol.* **274,** Pt 1, C1653–C1660
39. Deshpande, D. A., White, T. A., Guedes, A. G., Milla, C., Walseth, T. F., Lund, F. E., and Kannan, M. S. (2005) *Am. J. Respir. Cell Mol. Biol.* **32,** 149–156

40. Meszaros, L. G., Bak, J., and Chu, A. (1993) *Nature* **364,** 76–79
41. Protasi, F., Takekura, H., Wang, Y., Chen, S. R., Meissner, G., Allen, P. D., and Franzini-Armstrong, C. (2000) *Biophys. J.* **79,** 2494–2508
42. Flucher, B. E., Conti, A., Takeshima, H., and Sorrentino, V. (1999) *J. Cell Biol.* **146,** 621–630
43. Zhang, W. M., Yip, K. P., Lin, M. J., Shimoda, L. A., Li, W. H., and Sham, J. S. (2003) *Am. J. Physiol. Lung Cell Mol. Physiol.* **285,** L680–L690
44. Garssen, J., Van Loveren, H., Van Der Vliet, H., and Nijkamp, F. P. (1990) *J. Pharmacol. Methods* **24,** 209–217
45. Rosenberg, P., Hawkins, A., Stiber, J., Shelton, J. M., Hutcheson, K., Bassel-Duby, R., Shin, D. M., Yan, Z., and Williams, R. S. (2004) *Proc. Natl. Acad. Sci. U. S. A.* **101,** 9387–9392
46. Eu, J. P., Sun, J., Xu, L., Stamler, J. S., and Meissner, G. (2000) *Cell* **102,** 499–509
47. Zhao, F., Li, P., Chen, S. R., Louis, C. F., and Fruen, B. R. (2001) *J. Biol. Chem.* **276,** 13810–13816
48. Xu, L., Eu, J. P., Meissner, G., and Stamler, J. S. (1998) *Science* **279,** 234–237
49. Sun, J., Xin, C., Eu, J. P., Stamler, J. S., and Meissner, G. (2001) *Proc. Natl. Acad. Sci. U. S. A.* **98,** 11158–11162
50. Giannini, G., Clementi, E., Ceci, R., Marziali, G., and Sorrentino, V. (1992) *Science* **257,** 91–94
51. Hyvelin, J. M., Martin, C., Roux, E., Marthan, R., and Savineau, J. P. (2000) *Am. J. Respir. Crit. Care Med.* **162,** Pt 1, 687–694
52. Cabanes, L. R., Weber, S. N., Matran, R., Regnard, J., Richard, M. O., Degeorges, M. E., and Lockhart, A. (1989) *N. Engl. J. Med.* **320,** 1317–1322
53. Sutherland, E. R., and Cherniack, R. M. (2004) *N. Engl. J. Med.* **350,** 2689–2697
54. Barnes, P. J. (1997) in *The Lung: Scientific Foundations* (Crystal, R. G., West, J. B., Weibel, E. R., and Barnes, P. J., eds) pp. 1269–1285, Lippincott-Raven, Philadelphia
55. Janssen, L. J., Wattie, J., Lu-Chao, H., and Tazzeo, T. (2001) *J. Appl. Physiol.* **91,** 1142–1151
56. Nakai, J., Dirksen, R. T., Nguyen, H. T., Pessah, I. N., Beam, K. G., and Allen, P. D. (1996) *Nature* **380,** 72–75
57. Chavis, P., Fagni, L., Lansman, J. B., and Bockaert, J. (1996) *Nature* **382,** 719–722
58. Janssen, L. J. (2002) *Am. J. Physiol. Lung Cell Mol. Physiol.* **282,** L1161–L1178